Journal of Hydrology 617 (2023) 129007

Contents lists available at ScienceDirect

Journal of Hydrology

journal homepage: www.elsevier.com/locate/jhydrol

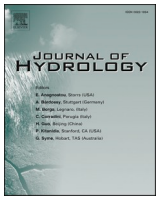

Research papers

Dynamic water level changes in Qinghai Lake from integrating refined ICESat-2 and GEDI altimetry data (2018–2021)

Zhijie Zhang [a,*], Yanchen Bo [b], Shuanggen Jin [c,d,e], Guodong Chen [a], Zhounan Dong [a]

[a] School of Geography Science and Geomatics Engineering, Suzhou University of Science and Technology, Suzhou 215009, China
[b] State Key Laboratory of Remote Sensing Science, Faculty of Geographical Science, Beijing Normal University. Beijing 100875, China
[c] Shanghai Astronomical Observatory Chinese Academy of Sciences, Shanghai 200030, China
[d] Nanjing University of Information Science & Technology, Nanjing 210044, China
[e] School of Surveying and Land Information Engineering, Henan Polytechnic University, Jiaozuo 454000, China

ARTICLE INFO

This manuscript was handled by Emmanouil Anagnostou, Editor-in-Chief, with the assistance of Guy Schumann, Associate Editor

Keywords:
GEDI laser altimetry
ICESat-2 ATL13
Qinghai Lake
Water level dynamics
Climate change

ABSTRACT

The water levels of inland lakes on the Tibetan Plateau are extremely sensitive to global climate change and can objectively reflect the temporal and spatial changes in local water resources. However, monthly and seasonal variations in lake water levels are difficult to monitor due to the lack of sufficient *in situ* gauges across mountainous areas. Moreover, GEDI products exhibit large uncertainties in mountainous surroundings. In this paper, taking Qinghai Lake as an example, we first refined the raw data of the GEDI and ICESat-2 missions by implementing a quality control procedure involving outlier removal tailored to the characteristics of each mission; then, we analyzed the accuracy of each mission, especially targeting factors that affect the water level retrievals in the GEDI products. Third, the bias between the two missions was adjusted by selecting the overlapping or adjacent observation dates. Finally, we constructed dense temporal water-level data by integrating the refined ICESat-2 and GEDI data. Data from water level stations and the DAHITI and Hydroweb datasets were also utilized for validation. The results show that (1) very accurate results can be obtained from the ICESat-2 ATL13 product, and the standard deviations of most observed days are under 0.05 m; (2) the GEDI products derived from algorithm 2 can offer more effective footprints than those from algorithm 1, with an improvement of approximately 9.78 %. Moreover, large differences exist among the different GEDI beams, and beams 1 and 2 are recommended for further analysis. Overall, most beams overestimated the lake levels with a bias of 0.264 ± 0.357 m; (3) the long-time-series water levels showed a mean increasing trend of 0.243 m/yr from 2018 to 2021. The relatively high-water-level periods were distributed mostly in August and September, while the low-water-level periods were distributed mostly in February and March. The combined water levels were very correlated with the DAHITI and Hydroweb datasets, with R values larger than 0.8, and highly consistent with the observations from hydrological stations (the inter-year change range spanned from 0.015 m to 0.327 m, and the intra-year difference range varied from 0.03 m to 0.16 m); and (4) Integrating the GEDI and ICESat-2 missions allowed us to capture the monthly, seasonal and annual dynamics of the lake water level, and the results indicate that the combined dataset presents a valuable resource for hydrological and climatic change studies.

1. Introduction

Water level fluctuations in endorheic lakes are sensitive to complex changes in regional precipitation, evapotranspiration, and glacier melting (Frappart et al., 2018; Kropáček et al., 2012; Talebmorad et al., 2020). Thus, the dynamics of inland lakes are not only significant parameters for understanding the water balance in interior drainage basins but are also valuable indicators of climate change. The Tibetan Plateau (TP) has the greatest number of high-elevation inland lakes in the world, and Qinghai Lake possesses the largest area among them; in addition, this lake is located in a typical area that is sensitive to climatic change and ecologically fragile (Wang et al., 2019; Javadinejad et al., 2019). Therefore, case studies of Qinghai Lake's water level changes are very important and valuable. However, due to the harsh natural physiographic and climatic conditions in this region, it is difficult to conduct field measurements over TP lakes; even if some are accessible,

* Corresponding author.
E-mail addresses: zjzhang@shao.ac.cn (Z. Zhang), sgjin@shao.ac.cn (S. Jin).

https://doi.org/10.1016/j.jhydrol.2022.129007
Received 25 May 2022; Received in revised form 9 November 2022; Accepted 15 December 2022
Available online 19 December 2022

continually performing measurements and maintaining *in situ* gauges are costly endeavors (Luo et al., 2021). Fortunately, the Global Ecosystem Dynamics Investigation (GEDI) mission can provide multi-track and high-temporal-resolution observations between the latitudes of 51.6° N and 51.6° S, and the advanced ICESat-2 that is the follow-up mission of the Ice, Cloud, and Land Elevation Satellite (ICESat) altimetry can also acquire unprecedented measurements of Earth's surface; these satellite missions have thus brought great prospects for lake level change monitoring.

In recent decades, satellite altimetry, including radar and laser altimetry, has been extensively applied to water level retrievals of inland water bodies (lakes, rivers, and reservoirs) (Talebmorad and Ostad-Ali-Askari, 2022; Busker et al., 2019; Crétaux et al., 2011; Velpuri et al., 2012). Initially, radar altimeters were developed to monitor sea and ocean surface topography. Because of their ability to provide precise water surface elevations over large water bodies, all-weather operability, and global data coverage, radar altimeter missions (such as Geosat, ERS-1/2, Topex/Poseidon, Envisat, Jason 1/2/3, Cryosat-2, and Sentinel-3 A and B) are being used increasingly often for monitoring and evaluating water surface height levels of inland water bodies (Birkett and Beckley, 2010; Calmant et al., 2008; Kleinherenbrink et al., 2014; Ghashghaie et al., 2022). However, the accuracy of such measurements can be affected by the extents of individual water bodies and by the retracking methods applied to returned waveforms (Guo et al., 2009; Wang et al., 2019). Compared to radar altimeters, laser altimeters have smaller footprints and higher sampling densities, making them more suitable for small-water-body observations. Many previous studies have investigated lake level changes over the TP using the geoscience laser altimeter system (GLAS) carried by ICESat with decimeter accuracy. Zhang et al. (2011) analyzed the lake level variations of Qinghai Lake and identified a mean increasing rate of 0.11 m/yr from 2003-2009. Phan et al. (2012) found an average change rate of 0.20 m/yr for 154 lakes (larger than 1 km^2). Moreover, by investigating the water levels of 105 closed lakes, Song et al. (2014) found that seasonal lake-level variations featured strong spatial and temporal heterogeneities.

ICESat-2 was launched in September 2018 and equipped with the Advanced Topographic Laser System (ATLAS), which is capable of detecting sensitivities at the photon level (Tian and Shan, 2021). The ATLAS instrument illuminates the Earth's surface with six ground tracks simultaneously. Laser footprints are typically approximately 14 m (in diameter), and the distance between two footprints along the track is only 0.7 m. Compared with GLAS, ATLAS can produce data at a much higher spatial resolution and denser sampling frequency. Zhang et al. (2019) found that ICESat-2 data contained nearly twice the lake coverage of TP lakes compared with ICESat data and also had a higher altimetric accuracy (the elevation difference was 2 cm at Lake Qinghai when compared to gauge data). Yuan et al. (2020) evaluated the altimetric precision of ICESat-2 ATL13 data using gauge data collected from 30 reservoirs and extensively studied large lakes (larger than 10 km^2) in China. Their work showed that the ICESat-2 mission greatly updated its altimetric capability, and the relative altimetric error was 0.06 m, while some mountainous and shallow lakes tended to have relatively large uncertainties. Dandabathula and Rao (2020) validated the ATL13 products with 46 observations consisting of near-real-time gauged data of 15 reservoirs and found that the maximum uncertainty observed was at the centimeter level.

The GEDI, launched on December 5th, 2018, started collecting scientific data in operational mode on March 25th, 2019, after a three-month on-orbit checkout. It was attached to the International Space Station and collected data globally between latitudes of 51.6° N and 51.6° S; the instrument can measure forest canopy heights, canopy vertical structures, and surface elevations to characterize important carbon and water cycling processes, biodiversity, and habitats (Adam et al., 2020). Fayad et al. (2020) analyzed the quality of GEDI data over 8 lakes in Switzerland and found that the bias between GEDI elevations and *in situ* data ranged from −13.8 cm to +9.8 cm. Xiang et al. (2021) validated and compared the GEDI, ICESat, and ICESat-2 data using *in situ* data from 22 gauging stations over the Great Lakes and lower Mississippi River and reported that the root mean square errors of the three missions were 0.28 m, 0.10 m, and 0.06 m, respectively.

With the goal of combining multiple altimeters for retrieving long-term lake level series, Wang et al. (2019) constructed the TOPEX/Poseidon-family altimeter dataset from October 1992 to December 2017, resulting in accuracies of ~17 cm for TOPEX/Poseidon and ~10 cm for Jason-1/2/3 over Ngangzi Co. Using Cryosat-2, Jason-2/3, and Sentinel-3A data, Chen and Liao (2020) determined that the level of Qinghai Lake had an increase rate of 0.443 m/yr from 2016 to 2019. When analyzing lake level changes in the middle and lower Yangtze River Basin using the long-term (2002–2017) observations of ICESat, Envisat, and CryoSat-2, the authors found that there was a significant correlation between the satellite altimetry water levels and measured water levels (with R values between 0.908 and 0.989, $P < 0.001$) (Li et al., 2020). By integrating ICESat/ICESat-2 data, the Global Surface Water dataset, and the HydroLAKES dataset, Luo et al. (2021) proposed plateau-scale research of lake level changes over the TP from 2003 to 2019. They reported 242 lakes with areas greater than 1 km^2 that could be observed by combining ICESat and ICESat-2 data, and the mean water level change rate of these lakes was 0.20 ± 0.04 m/yr. Frappart et al. (2021) provided a comprehensive evaluation of the performances of the previous radar and lidar altimetry missions according to their acquisition in mountainous areas and revealed that very accurate results could also be obtained using ICESat-2 data; however, more contrasting results were obtained when using GEDI in a relatively short period. Xu et al. (2022) revealed the seasonal trends and cycles of lake level variations over the TP by combining ICESat, ICESat-2, Sentinel-3A/3B, and Cryosat-2 data, demonstrating that Qinghai Lake rose at a rate of 0.17 ± 0.001 m/yr from 2003 to 2020.

In general, in the past two decades, the number of *in situ* hydrological stations in the world has declined (Lawford et al., 2013). Satellite altimetry is becoming an important tool for monitoring lake surface heights. However, lake surface level dynamic monitoring still faces many difficulties, such as large altimetric errors due to mixed signals contaminated by the surrounding lands, large spatial gaps between tracks, and temporal gaps that impede detailed variation descriptions. To date, the application and validation capacities of ICESat-2 and GEDI data over inland waters are very limited, as only 3 years of ICESat-2 data and 2 years of GEDI were accumulated at the time of their respective product releases. In particular, contradictory results have been obtained when applying GEDI data to study mountainous lakes. As ICESat-2 and GEDI are operating simultaneously, combining these two missions can provide a mutual accuracy verification and increase the temporal density of observations, allowing us to cope with temporal gaps in data. More analyses are necessary to determine the potential of using these missions to retrieve water levels. Therefore, the objectives of this paper are (1) to provide a robust strategy to delete outliers, generate accurate lake water levels from individual missions and analyze various factors that influence the accuracy of inland water level measurements derived from the GEDI laser altimetry platform; (2) to evaluate the performance of the combination of GEDI and ICESat-2 data in retrieving inland water dynamics; and (3) to track the latest dynamic water levels of Qinghai Lake. This paper is divided into five sections. A description of the altimetry datasets obtained for the studied lake and a detailed water-level extraction method are provided in Section 2. The individual water level results retrieved from both products and comparisons and validations of these data with the hydrostation data and two other public datasets are given in Section 3, followed by a discussion in Section 4. In the last section, the main conclusions are presented.

2. Data and methods

2.1. Altimetric data in Qinghai Lake

The latitude and longitude ranges of Qinghai Lake are 36°32′N −37°15′ N and 99°36′E −100°47′ E, respectively. As the largest inland lake in China, it is located on the northeast edge of the Qinghai Tibet Plateau. Located within the transition zone among the Qinghai Tibet alpine region, the Loess Plateau, and the northwest arid region, it is an ideal place to study climate responses, water balances, and hydrological processes (Zhao et al., 2017). In this study, we utilized the Level-2A GEDI product containing ground elevation, canopy top height, and relative return energy metrics derived from geolocated waveforms; the height data are based on the WGS 84 ellipsoid, and the inland surface water product ATL13 of ICESat-2 providing the along-track orthometric heights of lakes, rivers, and wetlands with reference to the Earth Gravitational Model 2008 (EGM2008) was obtained. When the first draft of this article was written, GEDI data from 25 April 2019 to 3 August 2021 and ICESat-2 data from 31 October 2018 to 3 July 2021 were available (https://search.earthdata.nasa.gov/). Among the current available data products, the higher-quality V002 version of the GEDI product and V004 version of the ICESat-2 product were adopted. The total available number of days in the GEDI and ICESat-2 datasets are 92 days and 76 days, respectively (Table 1). Among them, the highest observation frequency is 11 days in August 2020, while the observations frequencies of most months are 4–10 days. The specific laser footprints of the two missions were distributed over Qinghai Lake as shown in Fig. 2.

2.1.1. GEDI L2a

The GEDI instrument consists of 3 lasers producing a total of 8 ground-transect beams spaced approximately 600 m apart on the Earth's surface in the cross-track direction relative to the flight direction. Each beam transect consists of ~30-m-footprint samples spaced approximately every 60 m along the track. The "coverage" laser is split into two transects that are then each dithered in total, producing four ground transects. The other two full-power lasers are dithered, producing two ground transects each. The configuration of the ground tracks is shown in Fig. 1 (a) (Hofton et al., 2019); the instrument is a full-waveform lidar instrument that captures the shapes of the transmitted and reflected laser waveforms in real time. It enables a precise range to the reflecting surface to be calculated for every shot. Over flat terrain (e.g., plains or water surfaces), the shape of the received waveform looks similar to that of the transmitted pulse. However, photons may be reflected from multiple surfaces within the footprint over complex (e.g., stepped or sloped) terrain, resulting in a received waveform with multiple modes (Fayad et al., 2021). The interpretation of these laser pulses in post-processing affects the accuracy of the surface elevation, vegetation structure, relative canopy height results, etc. As mentioned in the Algorithm Theoretical Basis Document, the L1B product is issued by six configurations of algorithms (a1 to a6), each representing different thresholds and smoothing settings (Hofton et al., 2019). Correspondingly, the L2A geolocated elevation and height products inherit the results of these multiple algorithm settings. The N in the parameter 'elev_lowestmode_aN' represents the specific algorithm.

The position of the ground return within a waveform is determined using the position of the last detected peak, which is dependent on the width of the second Gaussian filter (Smoothwidth_zcross). The widths of algorithm 1 and 4 were fixed to 6.5 ns, and the widths of the remaining algorithms (2, 3, 5 and 6) were set to 3.5 ns (Fayad et al., 2020). Therefore, the six algorithms could be divided into two groups. In our study, only algorithm 1 (A1) and algorithm 2 (A2), which can represent each group, were tested. Moreover, GEDI uses its own global positioning system, inertial measurement unit, and information from three star-trackers that permit its plane positioning accuracy to remain within 10 m (1 σ) (Dubayah et al., 2020). The product contains a preliminary set of quality flags and metrics that can be used to filter shots with poor geolocation performances, waveforms of bad signal quality, and waveforms affected by clouds or other land surface conditions (Roy et al., 2021). Thus, the 'quanlity_flag_aN' flag and 'num_detectedmodes_aN' metric were adopted in our study to obtain accurate water level retrievals.

2.1.2. ICESat-2 ATL13

ICESat-2 is placed at a ~500-km altitude in a 92°-inclination sun-synchronous orbit with a 91-day repeat cycle and an equatorial ground-track spacing of approximately 28.8 km. The ATLAS instrument operates at a higher repetition rate, thus improving the along-track spatial resolution. ICESat-2 products are organized by ground track, with ground tracks 1L and 1R forming pair one, ground tracks 2L and 2R forming pair two, and ground tracks 3L and 3R forming pair three. The distance between the left and right beams of each pair is 90 m. Pair tracks are approximately 3 km and 2.5 km apart in the across-track and along-track directions, respectively (Fig. 1(b)) (Roy et al., 2021). The beams within each pair have different transmit energies, so-called weak and strong beams, with an energy ratio between them of approximately 1:4. The relative position of the strong and weak beams on the ground depends on the orientation of the ICESat-2 observatory, which changes approximately twice per year to maximize solar illumination (Neumann et al., 2020). Numerous subproducts generated from the Level 2 master product called ATL03 are available to the public through the National Snow and Ice Data Center. One of these products, namely, ATL13, provides along-track and near-shore water surface height distributions within the water masks, along with the mean, standard deviation, and slope of each beam as well as statistics (Jasinski et al., 2019). The water surface heights offer geodetic heights above the WGS 84 ellipsoid (ITRF2014 Reference Frame) and orthometric heights based on the Earth Gravitational Model 2008 (EGM2008) geoid.

2.1.3. Auxiliary data

In this study, the boundary of Qinghai Lake was determined from its year 2018 vector format file (shapefile), which was downloaded from the National Basic Geographic Information Centre (http://NGCC.SBSM.Gov.cn); the lake boundary was then used to extract elevation footprints. To unify the vertical data of ICESat-2 and GEDI, we used the EGM2008

Table 1
The altimetric data sampling days distribution in each month (ICESat-2 red notes and GEDI blue notes).

	Jan	Feb	Mar	Apr	May	Jun	Jul	Aug	Sep	Oct	Nov	Dec
2018										1d	1d	1d
2019	4d	3d	2d		2d/4d	1d/3d	2d/3d	4d/3d	3d/4d	3d/3d	3d/2d	4d/2d
2020	2d/6d	2d/1d	2d	2d/6d	3d/3d	3d/4d	2d/4d	3d/8d	2d/7d	3d/7d	2d	1d
2021	4d	3d	1d/5d	2d/5d	3d/5d	1d/5d	1d	1d				

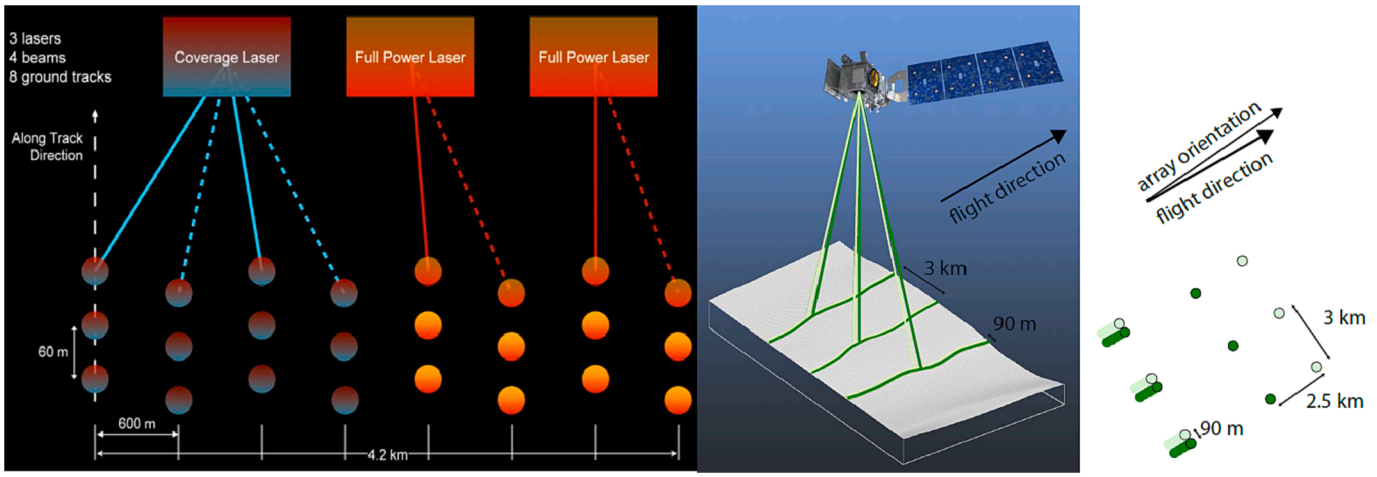

Fig. 1. Ground sampling pattern and tracks (beams) distribution of two missions: (a) GEDI; (b) ICESat-2(the figures were quoted from the Algorithm Theoretical Basis Document of each mission (Hofton et al., 2019; Neumann et al., 2020)).

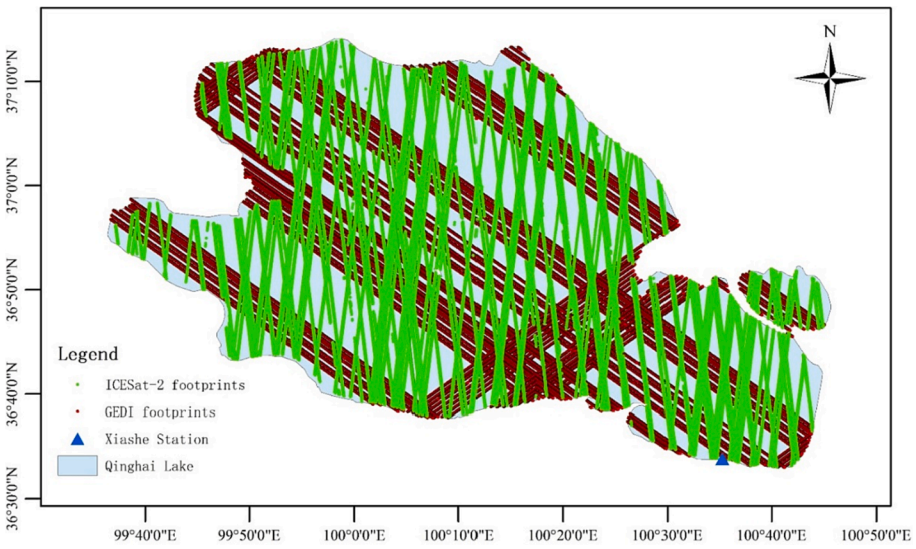

Fig. 2. Footprints distribution of GEDI and ICESat-2 over Qinghai Lake spanning from October 2018 to August 2021.

model to convert the GEDI heights based on WGS84 to heights based on EGM2008. The conversion software tools of the EMG2008 geoid model can be downloaded from the GeographicLib (htttps://geographiclib.sourceforge.io/html/geoid.html). In addition, to verify the integrated water level results, the available *in situ* gauge data of Xiashe station from 2018 to 2021 were collected from the Qinghai water conservancy information network (https://slt.qinghai.gov.cn/subject?cid=24). Time-series products from two other public databases were obtained to derive lake levels from multiple radar altimeters designed for inland water bodies, and these lake levels were used for comparison: the Hydrological Time-Series of Inland Waters (DAHITI) is maintained by the Deutsches Geodätisches Forschungsinstitut (Schwatke et al., 2015), and the Hydroweb database is constructed by the Laboratoire d'Etudes en Géophysique et Océanographie Spatiales (Yue et al., 2021). The elevation reference data were the GGM02C and EIGEN-6C4 gravity field models.

2.2. Water level extraction

Fig. 3 depicts the processing steps in the proposed method. First, the laser footprints over Qinghai Lake were roughly extracted using the lake boundary. Then, the outlier deletion of each mission was implemented. Subsequently, the water level at each track was extracted, and the corresponding accuracy assessment was conducted. The effective tracks were then used as the inputs on specific dates, and the final heights of each mission were estimated by calculating averages. To evaluate the lake level accuracies of the two missions, the standard deviation was selected to assess the single-track and mean lake levels of each individual day derived from the effective tracks. Before integration, the bias between the two missions was adjusted using data from the overlapping or adjacent dates. Finally, the long-time-series lake levels and corresponding accuracies were constructed and validated using the *in situ* data and the DAHITI and Hydroweb datasets.

2.2.1. Outlier detection

Due to the effects of atmospheric conditions and clouds, not all altimetric observations are effective (Hui et al., 2016). Therefore, outliers should be removed before estimating the mean lake levels. For example, the height distributions of 8 GEDI beams on 12 Sep 2019 (Fig. 4(a)) and 6 ICESat-2 tracks on 7 Sep 2019 (Fig. 4(b)) illustrate that the height differences among different GEDI beams are larger than the differences among ICESat-2 tracks, and the GEDI data contain many extreme outliers, while the ICESat-2 data have small differences among different tracks and few extreme outliers. Thus, in this study, a

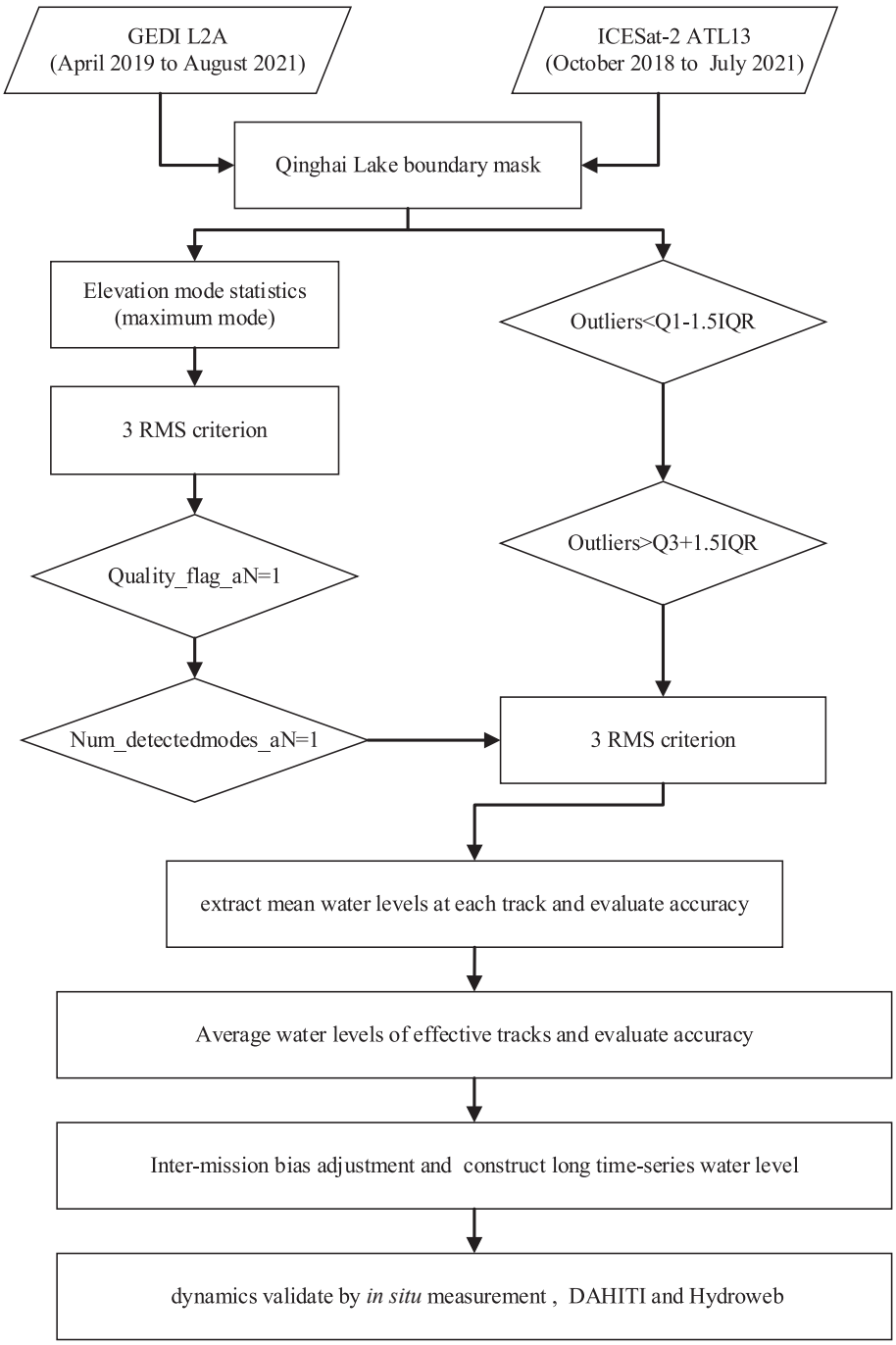

Fig. 3. The flowchart of GEDI and ICESat-2 refinement over Qinghai Lake spanning from October 2018 to August 2021, and the construction and validation of long time-series water levels.

combination of criteria was applied to remove outliers according to their characteristics.

For GEDI L2A, in the first step, the quality flag (quality_flag_aN) and mode number flag (num_detectedmode_aN) contained in the products were used. A quality_flag_aN term the value equal to 1 indicates that the waveforms met the energy, sensitivity, amplitude, and real-time surface tracking quality criteria. Then, the num_detectedmode_aN flag value of 1 was selected to guarantee that the waveform returned from the lake surface. Second, the estimation of the elevation bin with 1 interval was implemented. A step size of 1 m was used to address the water surface slopes associated with various causes. The lake water heights within the maximum bin that possess the highest frequency were preserved. The rest outside the 1 m interval from the maximum bin were discarded as outliers. Third, the mean water level was calculated based on the remaining heights, and the root mean square (RMS) values of the residuals between the heights and the mean water level were estimated. The values were considered outliers if the absolute differences between the observations and the mean water level were greater than the 3-RMS criterion. Finally, even if a single beam met the above requirements, if the differences among different beams on the same day were larger than 1 m, the mean value of the beams of the specific day was removed due to the large uncertainty.

For ICESat-2 ATL13, the interquartile range (IQR) was adopted. The height outliers were defined using Eqs. (1) and (2). Then, the 3-RMS criterion was applied, in case the first step did not work well. Eqs. (1) and (2) are expressed as follows:

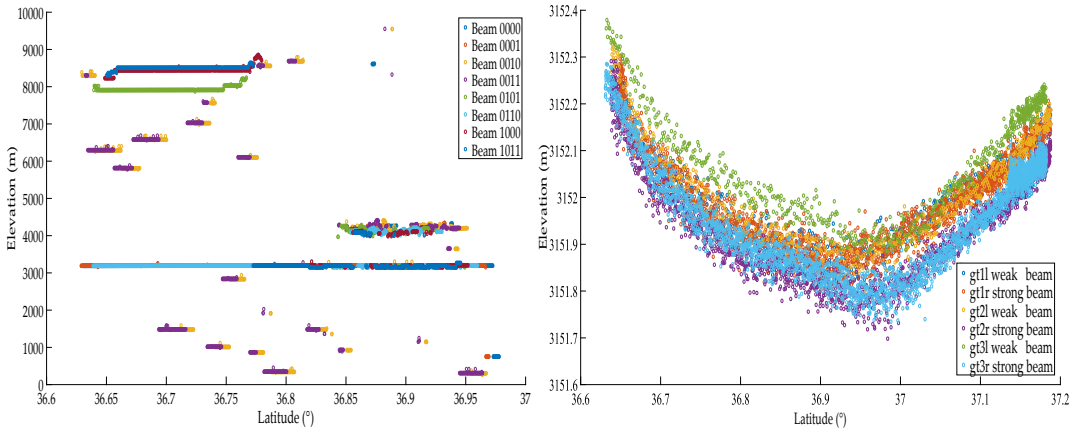

Fig. 4. Examples of GEDI and ICESat-2 geodetic heights distribution along with latitudes: (a) GEDI; (b) ICESat-2 (The height reference is based on WGS84).

$$IQR = Q_3 - Q_1 \tag{1}$$

$$\begin{cases} H_{outlier} < Q_1 - 1.5IQR \\ H_{outlier} > Q_3 + 1.5IQR \end{cases} \tag{2}$$

where Q_1 is the first quartile, Q_3 is the third quartile, and $H_{outlier}$ is the abnormal height.

2.2.2. Inter-mission bias adjustment

It is very important to adjust the biases between different missions before combining multi-mission data and constructing time-series records. Absolute calibration using tide gauge data is the most common method (Schwatke et al., 2015). To avoid interference with altimetric signals, the fixed stations should be far enough from land and small enough such that the site does not impede the altimeter response; otherwise, the method may be unusable when measured data at fixed sites are lacking. In addition, two other methods, crossover analysis and collinear analysis, have also been employed to adjust the inter-satellite bias for global and regional studies (Bosch et al., 2014). However, *in situ* gauge stations and simultaneous crossover points are not available for most lakes, so these two methods were not options in this study. In this paper, a simple relative calibration method was employed to estimate the bias between the GEDI and ICESat-2 datasets. Assuming that the surface of a lake is a flat plane, the lake levels observed by mission A should ideally be equal to those simultaneously measured by mission B. However, because of the existence of bias and noises such as waves and seiches, these differences are not equal zero in reality and are calculated as follows:

$$\Delta_i = H_i^A - H_i^B \tag{3}$$

where $i = 1, 2, \cdots, K$ represents the number of pair samples in the overlapping period of the two missions; Δ_i is the difference between the pair samples; and H_i^A and H_i^B are the water levels observed by GEDI and ICESat-2, respectively.

Generally, two missions do not overfly the same lake in the same epoch. Therefore, to ensure that there are enough pair samples to accurately estimate the bias, we broadly selected the data taken on the same or adjacent days for the bias adjustment process. Because interpolation among adjacent days might introduce interpolation errors when calculating the differences, we assumed that the lake level would not change suddenly among most adjacent dates; thus, in our study, we did not consider interpolation effect. In addition, Xiang et al. (2021) compared water level retrievals from ICESat-2 and GEDI, as well as ICESat-1, and validated them against *in situ* data from 22 gauging stations at various scales in the Great Lakes; the results showed that ICESat-2 can provide lake water level retrievals with an unprecedented accuracy (RMSE = 0.06 m, biases = 0.01 ± 0.05 m). Thus, if the differences between the pair samples are larger than 1 m, the observation result of ICESat-2 is taken as the water level of that day, and the GEDI observation results are discarded as abnormal values. Supposing the remaining differences obey a normal distribution, the biases can be estimated from these differences using the maximum likelihood estimation method.

2.2.3. Accuracy assessment and validation

Altimetric errors can be quantitatively calculated when gauge water levels are available. However, gauge data are not accessible from most lakes in high-elevation areas. Therefore, in this study, the standard deviation (SD) of the mean water level height was taken as an indicator of the altimetric uncertainty to present the measurement error of the estimated water levels. Considering that the final lake water level was calculated from multi-beam observations taken over the water surface, the final lake water level would be precise if the measurement uncertainty was low. To validate the accuracy of the water level extraction results, the monthly and yearly changes of the available *in situ* gauge data of Xiashe station, DAHITI, and Hydroweb database were compared and the differences were analyzed.

3. Results and analysis

After outliers were removed, the water levels of Qinghai Lake from October 2018 to August 2021 were derived from the two missions. Since no *in situ* gauge data of each GEDI observation day were available for absolute validation, ICESat-2 data were employed as the benchmark for the following validation and calibration of lake levels resulting from the GEDI mission. First, the processing algorithm, acquisition time, and beam intensity of the GEDI data that may have affected the water levels were discussed and quantitatively analyzed. Then, the biases between the two missions were adjusted, and long-time-series monthly lake-level time series were constructed.

3.1. Lake levels retrieved by ICESat-2

Fig. 5 displays the water level dynamics and SDs retrieved from each ICESat-2 observation. The lowest water level of 3196.87 m occurred on 3 Dec 2018, and the highest water level of 3197.99 m occurred on 2 Oct 2020. In 2019, the water levels presented an increase from January until August, when the lake reached its maximum water level, and then declined in September, before increasing again in October and November and finally declining in December. A similar trend occurred in 2020. Generally, the water level of Qinghai Lake has increased over the last three years. The SDs of most days were under 0.05 m, and the mean SD of all observations was 0.03 m. Therefore, the water levels of ICESat-2 could be taken as the benchmark to evaluate the GEDI observation results.

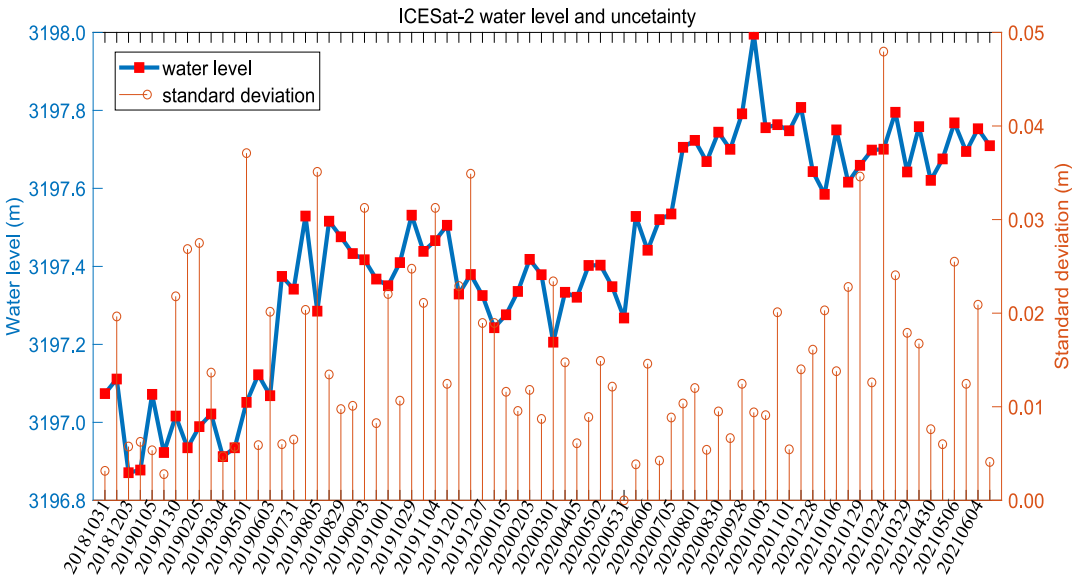

Fig. 5. Time-series lake water levels retrieved by ICESat-2 ATL13 and its uncertainty.

3.2. Lake levels retrieved by GEDI

3.2.1. Algorithm 1 versus algorithm 2

After removing the outliers, we found 59 days and 68 days effectively measured via algorithm A1 and A2, with effective rates of 64.13 % and 73.91 % of the total 92 GEDI days, respectively; In the common 59 days obtained by both algorithms, the differences of the retrieved water levels between algorithm 1 and algorithm 2 were extremely small, with a mean value of approximately −1 cm (Fig. 6), meaning that there were basically no differences between the lake water level retrieval results. The mean SDs of the corresponding retrieval results were 0.09 m and 0.12 m, respectively. Among the effective days obtained using algorithm 1 and algorithm 2, the numbers of days on which all 8 beams collected valid data were 30 days and 50 days, accounting for 50.84 % and 73.53 % of the total, respectively. Since there is no significant difference between the water level inversion results and accuracy, and the algorithm 2 has more effective data, in this paper, we selected the results of algorithm 2 for the following analysis.

3.2.2. Daytime observation versus nighttime observation

The results from algorithm A2 were grouped by time: the temporal range from 8:00 to 20:00 was considered daytime, and the rest of the 24-hour cycle was considered nighttime. Fig. 7 shows the SD comparison of the GEDI daytime and nighttime observations. The results showed that the SDs varied from 0.018 m to 0.312 m for the 38 days acquired in the daytime, with a mean SD of 0.115 m. For the 30 days acquired in the nighttime, the SDs spanned from 0.019 m to 0.295 m with a mean of 0.110 m. Overall, from the perspective of the average error, the influence of the observation time on water levels showed little difference between daytime and nighttime.

3.2.3. Coverage beams versus full-power beams

To examine the influence of the beam strength on the accuracy of the water level observations, the SDs of different beams were analyzed. The mean water levels were computed from the coverage beams (beam 0000, beam 0001, beam 0010, and beam 0011 were marked 1, 2, 3, and 4 in turn) and full-power beams (beam 0101, beam 0110, beam 1000, and beam 1011 were abbreviated as 5, 6, 7 and 8 in turn). Among the 68 days considered, the numbers of lacking-data days were 11 days for the

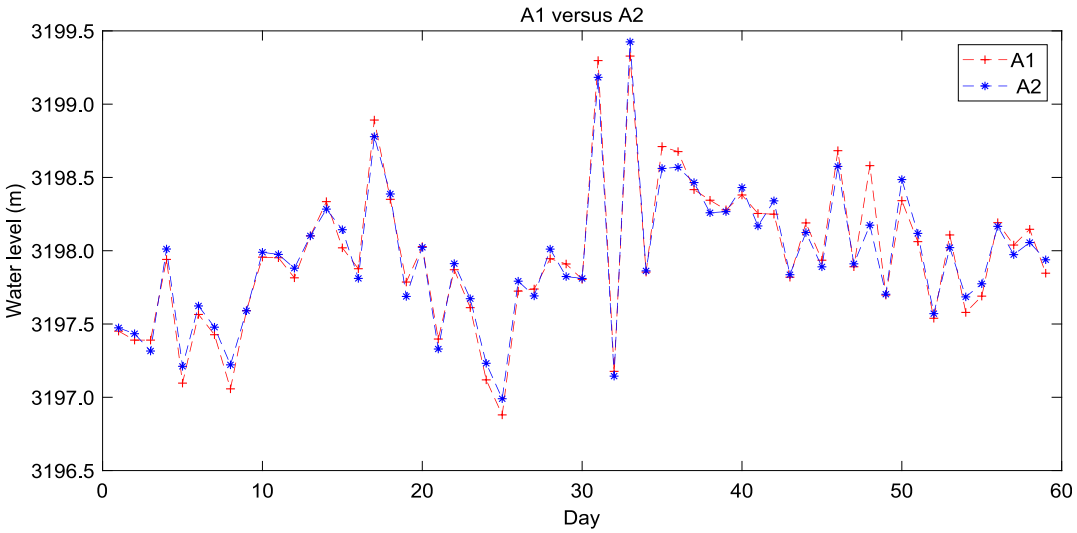

Fig. 6. Comparison of lake water levels retrieved by common days of GEDI algorithm 1 and algorithm 2.

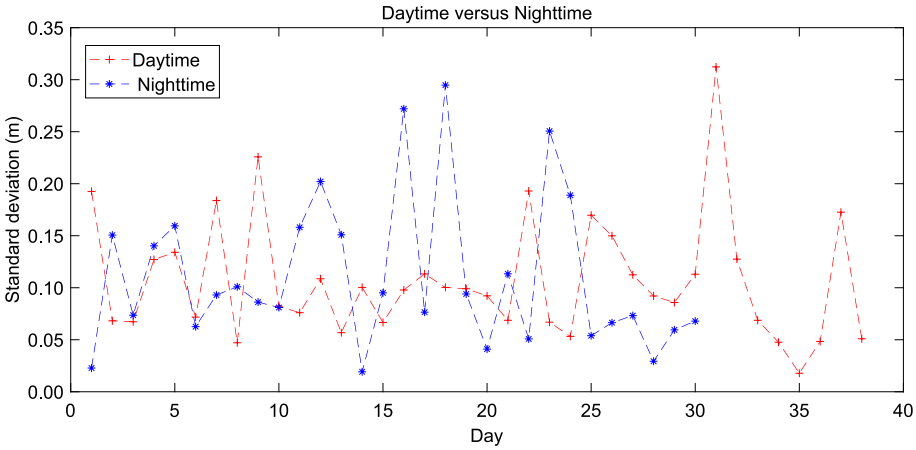

Fig. 7. The comparison between standard deviations of daytime and nighttime of algorithm A2.

coverage beams and 2 days for the full-power beams. Fig. 8 shows the SD comparison of the coverage beams and full-power beams, showing that the SDs of the coverage beams were generally larger than those of the full-power beams. The average SDs of the coverage-beam and full-power-beam results were 0.116 m and 0.100 m, respectively. The number of days with full-power-beam observations and the corresponding SDs revealed that the strong beams obtained more effective observations and had higher accuracies than the weak beams. Furthermore, Fig. 9 illustrates the differences between each GEDI beam and ICESat-2 track that were observed with the same or adjacent dates. The specific mean differences between each beam and the ICESat-2 results were 0.104 m, 0.054 m, 0.212 m, 0.214 m, 0.260 m, 0.293 m, 0.170 m, and 0.109 m. As a result, systematic differences were identified among the different beams, and the largest biases occurred in beams 3, 4, 5, and 6, followed by beams 7 and 8; beams 1 and 2 had the smallest biases.

3.3. Bias adjustment between GEDI and ICESat-2

Twenty-two paired samples were found in the overlapping observations (obtained on the same or adjacent days) between the GEDI and ICESat-2 datasets. From Table 2, it can be seen that there were 4 days with same-date observations, and the intervals between the remaining instances were 1–5 days. Fig. 10 visually displays the differences between the GEDI and ICESat-2 datasets. The red dots are outliers that should be removed before estimating the mean bias. The mean bias and SD are represented by the green and red dashed lines, respectively. Compared to ICESat-2, the negative difference of 4 days means that these GEDI underestimated the lake levels on these observation days; the rest are all positive, meaning that most GEDI observations reflected overestimated water levels. There were 3 days on which the differences were larger than 1 m (October 6 and December 1 in 2019 and June 26 in 2020, on which significant differences of 1.704 m, 1.449 m, and 1.663 m, respectively, were observed). According to the bias adjustment principle discussed above, the corresponding GEDI-observed values were deleted as abnormal records, and the ICESat-2-observed values were thus kept as the water levels of the corresponding days. The mean bias of the remaining 19 days was 0.264 ± 0.357 m, revealing that GEDI overestimated the water levels. Therefore, the adjusted GEDI lake levels were calculated by subtracting the mean bias from the original values.

3.4. Obtaining and validating long-time-series lake levels by integrating GEDI and ICESat-2 datasets

Fig. 11 illustrates the integrated lake water level dynamics (the red crosses mark the adjusted GEDI results) and their corresponding SDs for the specifically acquired days spanning from October 2018 to July 2021. It can be seen that the combined dataset significantly densified the monitoring time compared to each mission alone. From the water level

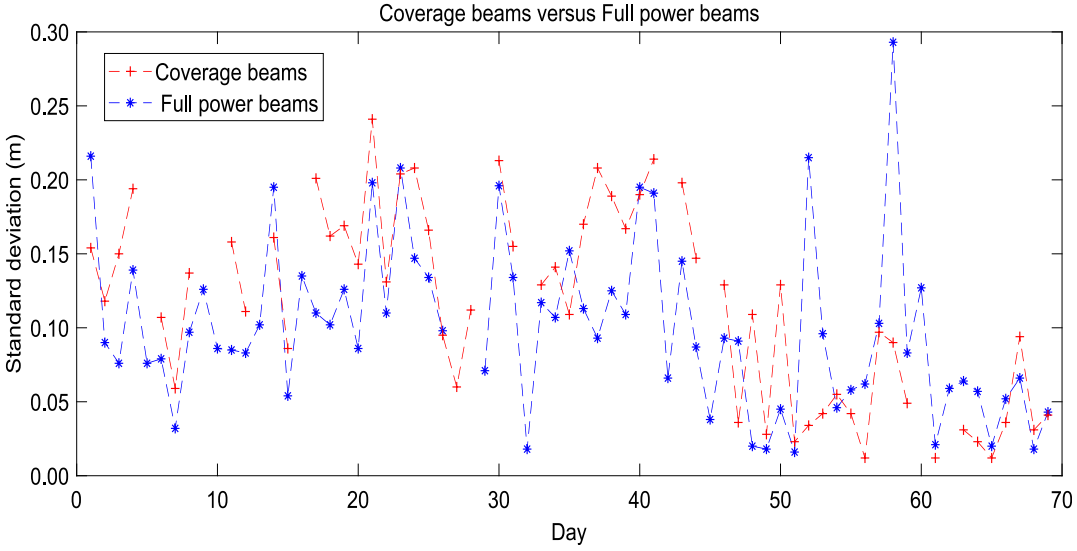

Fig. 8. The standard deviation comparison between coverage beams and full power beams of GEDI.

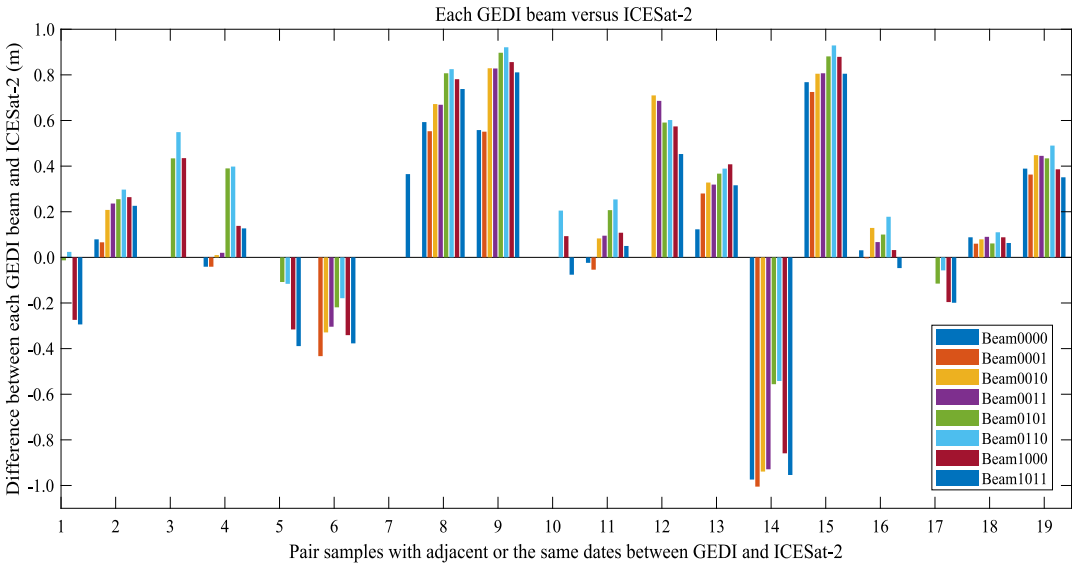

Fig. 9. The comparison between each beam of GEDI and ICESat-2 with same or adjacent dates.

Table 2
The sample pairs with the same or adjacent dates acquired by GEDI and ICESat-2 missions.

Dates	ICESat-2 average (m)	Dates	Times	GEDI A2 average(m)	Differences (m)	Delta days
20190501	3197.051	20190502	023839	3197.434	0.383	1
20190510	3197.122	20190508	235552	3197.316	0.194	2
20190603	3197.068	20190606	123324	3197.211	0.143	3
20190711	3197.374	20190712	221016	3197.478	0.104	1
20190809	3197.516	20190811	032443	3197.221	−0.294	2
20190829	3197.476	20190829	200012	3197.990	0.514	0
20190907	3197.367	20190912	211407	3197.975	0.607	5
20191006	3197.410	20191009	104136	3199.113	1.704	3
20191108	3197.505	20191109	153117	3198.143	0.638	1
20191201	3197.329	20191201	133657	3198.778	1.449	0
20200128	3197.336	20200126	090346	3197.912	0.576	2
20200405	3197.321	20200406	050300	3197.232	−0.089	1
20200428	3197.321	20200429	194548	3198.011	0.690	1
20200502	3197.403	20200503	181134	3197.824	0.421	1
20200504	3197.348	20200507	163718	3197.811	0.463	3
20200629	3197.520	20200626	035415	3199.183	1.663	3
20200728	3197.705	20200728	081942	3197.144	−0.561	0
20200830	3197.744	20200901	181701	3198.569	0.825	1
20210329	3197.642	20210329	074921	3197.703	0.061	0
20210506	3197.768	20210510	214734	3197.627	−0.142	4
20210529	3197.695	20210526	153558	3197.774	0.080	3
20210604	3197.753	20210603	123028	3198.166	0.413	1

of an individual day, except for several relatively high adjusted water level days retrieved by GEDI, the overall days constituting the relatively high-water-level periods were distributed mostly in August and September, followed by October and November, while the days constituting relatively low-water-level periods were distributed mostly in February and March. Overall, the water levels showed upward trends.

Assuming that the yearly water levels in 2018 and 2021 could be roughly expressed with observed months, the annual average water levels for 2018, 2019, 2020 and 2021 were 3197.019 m, 3197.252 m, 3197.607 m, and 3197.748 m, respectively. Compared to each previous year, the yearly increases were 0.233 m 0.355 m and 0.141 m. The reference average annual growth value from 2018 to 2021 was 0.243 m/yr, which should represent an underestimation of the yearly increasing rate due to the lack of data on the higher-level 2021 season. The corresponding annual average water level data from the Xiashe water level station showed water levels of 3195.41 m, 3195.97 m, 3196.34 m and 3196.51 m, showing increases of 0.56 m, 0.37 m and 0.17 m compared to each previous year. The corresponding average annual increase was 0.367 m/yr. Overall, from the perspective of inter-annual changes, it can be seen that the water level of Qinghai Lake showed an upward trend over the four years of study.

To further evaluate the validity of our integrated results, we used monitoring data from the DAHITI and Hydroweb databases. The water levels and the uncertainty of each individual day are shown in Fig. 12. For the inter-year changes from 2018 to 2021, the increases in DAHITI were 0.539, 0.318 m and 0.146 m, with a mean rate of 0.334 m/yr, and those in Hydroweb were 0.416 m, 0.444 m and 0.216 m, with a mean rate of 0.359 m/yr. To compare the three datasets, the days with same-day observations or with an interval of two adjacent days were selected. From Fig. 13 (a), it can be seen that our combined results acquired more data in a relatively short period, and their water levels all presented upward trends from 2018 to 2021. The subfigure in the bottom right-hand corner displayed the change trend of the common eight days among these three datasets, demonstrating their good consistency. Fig. 13 (b) and (c) further illustrate the correlations (R values) between our results and the other two datasets. The overlapping days in the

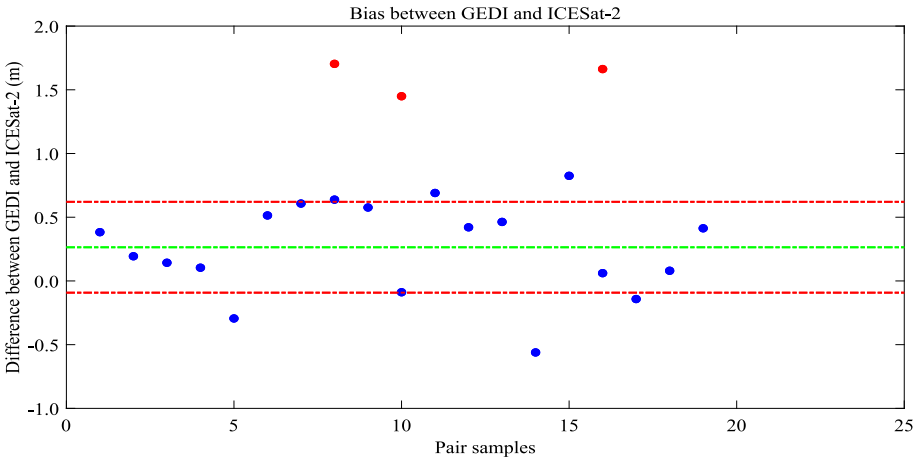

Fig. 10. Differences between 22 pair samples of GEDI and ICESat-2 missions (Red dots are outliers; the green dashed line and the red dashed lines represent mean bias and SD). (For interpretation of the references to colour in this figure legend, the reader is referred to the web version of this article.)

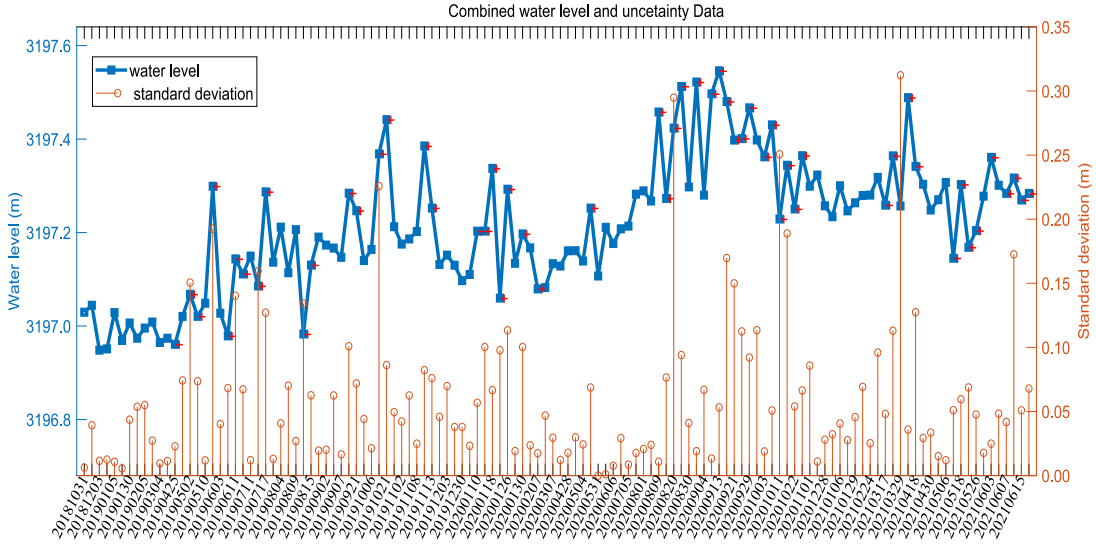

Fig. 11. The mean and standard deviation of lake water level retrieved by integrating GEDI and ICESat-2 (the red cross marked adjusted GEDI results). (For interpretation of the references to colour in this figure legend, the reader is referred to the web version of this article.)

DAHITI and Hydroweb datasets were 41 and 17, respectively, and the R values of both exceeded 0.8, indicating the validity of our monitoring results.

Fig. 14 further compares and analyses the inter-annual and intra-annual differences among the four data sources. Compared to the Xiashe station (Fig. 14 (a)), the differences between our results, the DAHITI dataset, and the Hydroweb dataset and the gauge data were −0.33 m, −0.02 m, and −0.14 m, respectively, from 2018 to 2019. The large difference between our results and the water station data from 2018 to 2019 may have been caused by the lack of data in the first three seasons of 2018. However, the corresponding differences were −0.02 m, −0.06 m, and 0.08 m, respectively, from 2019 to 2020, indicating that our retrieved results were more consistent with the gauging station data in this period. The differences for 2020 to 2021 were −0.06 m, −0.02 m and 0.05 m, respectively. The relatively small difference increase can be attributed to the limited data in 2021. Because 2019 and 2020 have complete whole-year observation data, we compared only the intra-year changes during these two years (Fig. 14 (b)). For 2019, the water levels revealed by our integrated results at the beginning and end of 2019 were 3196.972 m and 3197.319 m, respectively, with an increase of 0.347 m throughout the year. The corresponding levels from Xiashe station were 3195.71 m and 3196.09 m, respectively, and the water level rose by 0.38 m. The difference was −0.03 m, indicating that the integrated water levels were highly consistent with those measured at the hydrometric station. The increases in the DAHITI and Hydroweb data were 0.364 m and 0.500 m, with differences from the Xiashe station data of −0.02 m and 0.12 m, respectively. In 2020, the yearly increases in our results, the Xiashe station data, the DAHITI dataset and the Hydroweb dataset were 0.163 m, 0.32 m, 0.376 m, and 0.550 m, respectively; the differences between the three datasets and the Xiashe station data were −0.16 m, 0.06 m and 0.23 m, respectively. Obviously, the increase from the beginning to the end of each year was relatively small in our results, which may have been affected by the fact that most of the dates used to retrieve the average water level in January came from GEDI (Table 1), which overestimated the early-season water levels.

Fig. 15 shows the monthly average water levels. From the intra-annual changes in 2019, it can be seen that the lake water levels in January and February were relatively high before declining in March and subsequently gradually increasing from April to October; compared to the May and July levels, there was a downward fluctuation throughout June and August before the water level again reached higher levels in September and October. Finally, in winter (November and December), the water level dropped again. The year 2020 presented similar characteristics and trends: relatively low water levels occurred in

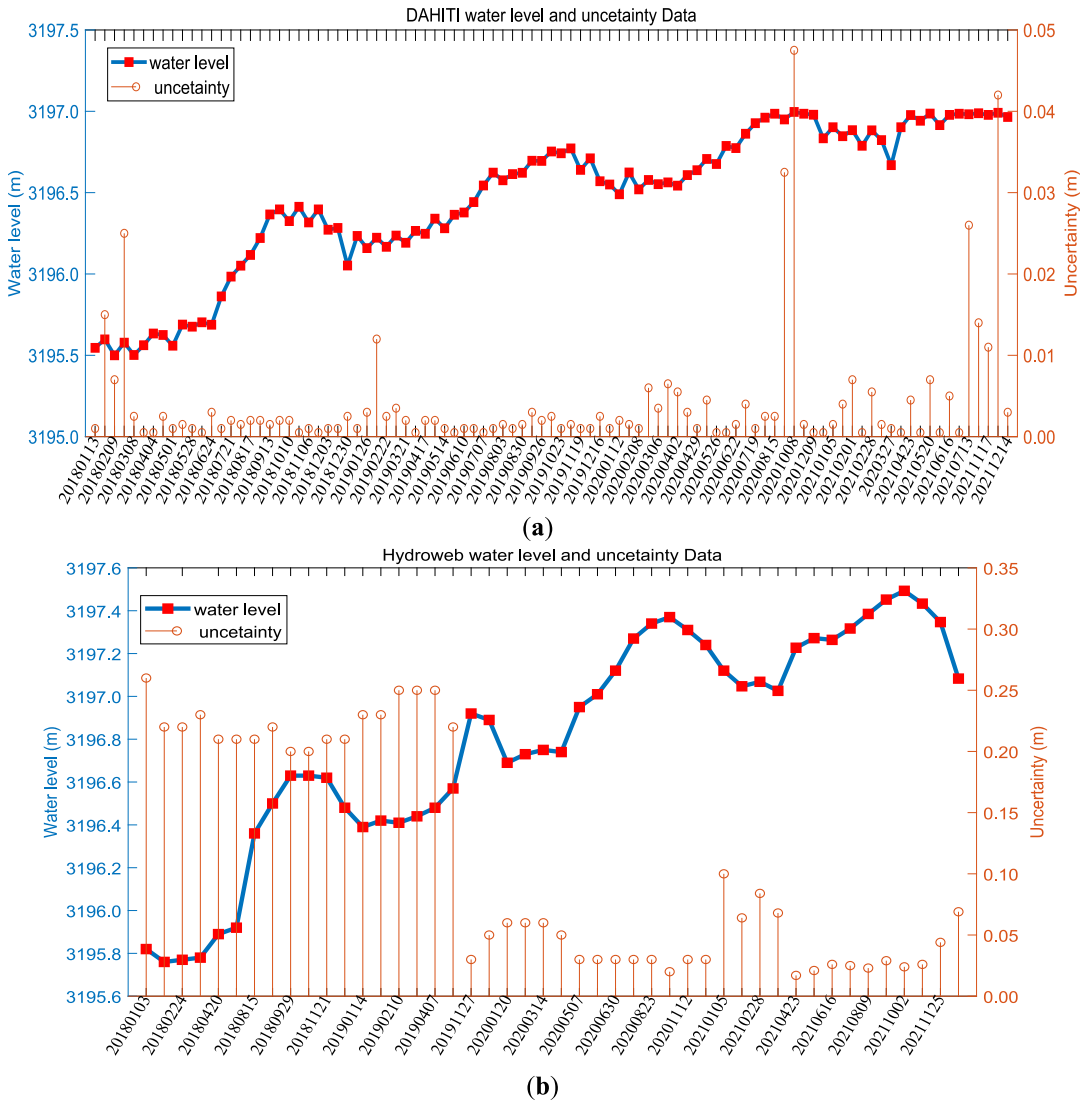

Fig. 12. Time-series water levels and their uncertainty of Qinghai Lake from two public datasets: (a) DAHITI; (b) Hydroweb.

February and March, while higher water levels occurred in August, September and October. However, there was an upward trend from February to April and a downward trend from May to July in 2021. On this basis, we also calculated statistics on seasonal changes. From October to December, the average water levels each year from 2018 to 2020 were 3197.019 m, 3197.598 m and 3197.799 m, exhibiting increase rates of 0.580 m/yr and 0.202 m/yr, respectively. The increase rates in the first three quarters of each year from 2019 to 2020 were 0.423 m/yr, 0.491 m/yr, and 0.602 m/yr. Compared to 2020, the increase rates in the first two quarters of the 2021 year were 0.342 m/yr and 0.140 m/yr.

The corresponding monthly, seasonal and annual variations in the DAHITI and Hydroweb datasets were also analyzed (Fig. 16). Comparing the 2019 and 2020 data in Fig. 15 with those in Fig. 16, our results presented the variations within all months of the year; however, the DAHITI product lacked data for one month in 2020, and the Hydroweb dataset lacked records for half a year in 2019 and for one month in 2020, indicating that combining the ICESat-2 and GEDI datasets can reflect more detailed temporal changes. Excluding elevation deviations due to the instrument biases of altimeters and geoid differences, it can be seen that the water levels of both datasets reflected rising trends over the last four years. Relatively high-water level occurred in September and October, while low water levels occurred in February and March; these trends were consistent with our research results.

However, obvious subseasonal differences occurred among the datasets. For example, in 2019, our data showed a downward trend from January to April, where an upward trend could be observed in both the DAHITI and Hydroweb datasets. A similar difference occurred in 2021, when our results indicated an increase from January to March while the DAHITI and Hydroweb datasets indicated decreases. Comparing to the results obtained for the month of April, neither of the two other datasets showed any large increase in May; however, our results showed a decline of approximately 0.265 m.

4. Discussion

When retrieving lake levels, whether directly using satellite altimetric data or integrating other remote sensing data, the key is to accurately extract the effective footprints over lakes and evaluate the accuracies of both the original data and extracted results. In this paper, we combined data from two newly launched laser altimetry missions, GEDI and ICESat-2, to monitor lake water level dynamics over the Tibetan Plateau area. Specifically, taking Qinghai Lake as an example, we obtained the daily, monthly, seasonal and yearly lake level variations from 2018 to 2021 from the GEDI L2A data product and ICESat-2 ATL13 product. From the above results, two aspects could be further

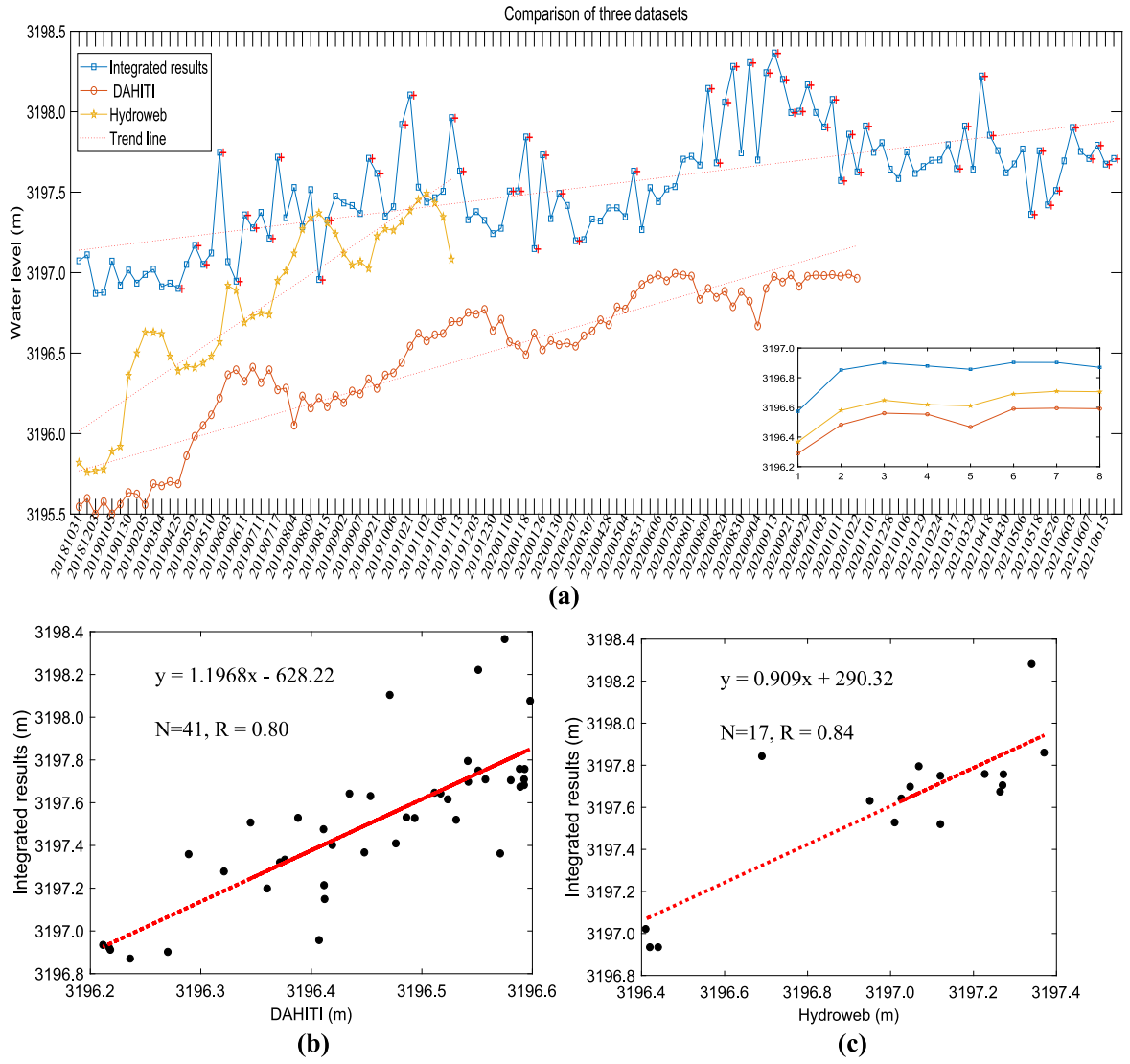

Fig. 13. The comparison and cross validation of three datasets (the red dotted line is the trend line): (a) comparison of three datasets and the common days acquired at the same day or with an interval of two days (The x-axis time is based on our integrated data); (b) correlation between the integrated results and DAHITI; (c) correlation between the integrated results and Hydroweb. (For interpretation of the references to colour in this figure legend, the reader is referred to the web version of this article.)

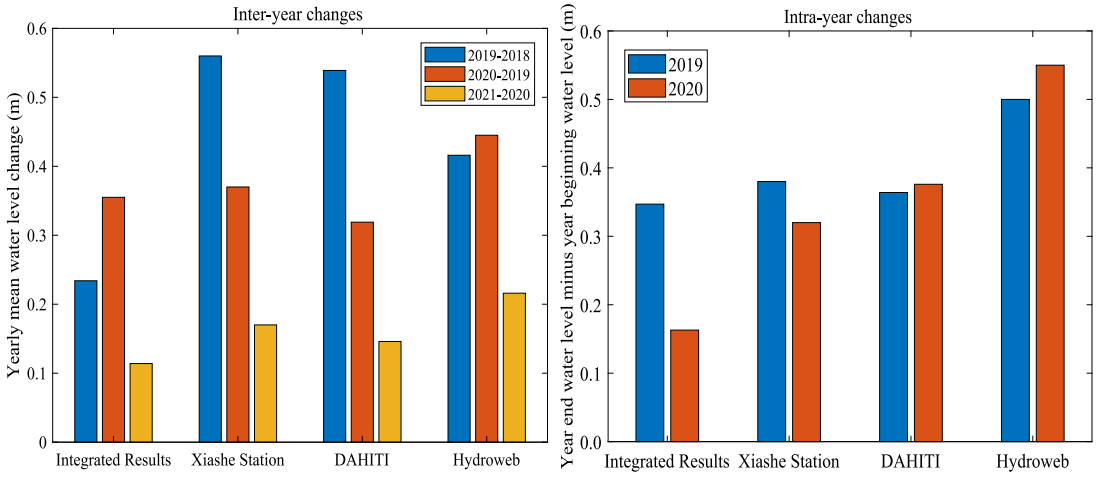

Fig. 14. Annual growth comparison of the intra-year and inter-year changes: (a) annual growth from year 2018–2019, 2019–2020 and 2020–2021; (b) intra-annual growth of year 2019 and 2020.

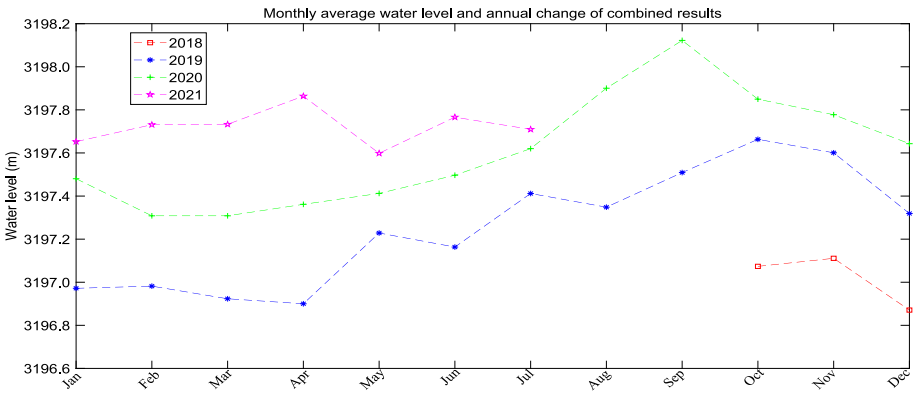

Fig. 15. The monthly average lake water level in the year 2018, 2019, 2020 and 2021.

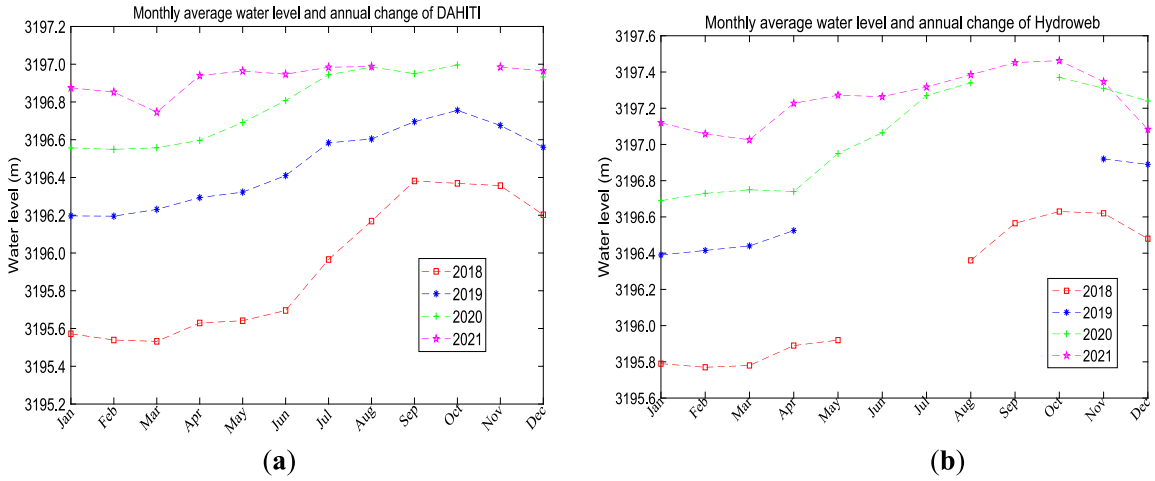

Fig. 16. Average water levels of each monthly and yearly variation of Qinghai Lake: (a) DAHITI; (b) Hydroweb.

investigated in future research. First, the accuracy of the current results should be improved, as discussed in Part 4.1. Second, the results and the factors that potentially caused the observed lake level changes should be linked, as described in Part 4.2.

4.1. Factors affecting the lake level extraction accuracy

The SDs of the GEDI data ranged from 0.018 m to 0.312 m, with an average of 0.109 m (Fig. 11). Because GEDI overestimated the water levels even after the bias adjustment, the GEDI's overall water levels were relatively high, and the SDs were larger than those of ICESat-2. For example, the maximum GEDI-measured water level of 3198.365 m occurred on September 13, 2020, and the maximum SD of 0.312 m occurred on March 29, 2021. For the integrated total of 126 days, the SDs spanned from 0.005 m to 0.312 m with an average of 0.061 m. For most dates, the SDs were below 0.20 m. The specific dynamics of the individual days and uncertainties in the DAHITI and Hydroweb datasets are shown in Fig. 12. Fig. 12(a) indicates that the DAHITI dataset had dense data and a high precision. The uncertainty in this dataset ranged from 0.001 m to 0.095 m with a mean value of 0.008 m. Hydroweb presented relatively sparse data (Fig. 12(b)) with relatively large uncertainties in 2018 and the first half of 2019, with the whole uncertainty range spanning from 0.017 m to 0.260 m with a mean of 0.113 m. Compared to the results obtained from DAHITI, the accuracy of our integrated results still needed to be further improved.

In addition, our results and methodology were compared to the recent results and approaches of Yuan et al. (2020) and Fayad et al. (2020), who evaluated the performances of the ICESat-2 and GEDI datasets, respectively, with *in situ* data. Compared to their work, we performed a more rigorous method to remove outliers. In addition, the IQR, 3 Sigma criterion, and quality flags were also adopted to derive more accurate water levels with an average SD of 0.03 m for ICESat-2 and an average SD of 0.109 m for GEDI. The relative altimetric error and uncertainty of ICESat-2 were reported to be 0.06 m and 0.02 m, respectively (Yuan et al., 2020), and in Fayad et al. (2020), the biases between the GEDI elevations and *in situ* data of eight studied lakes ranged from −13.8 cm to +9.8 cm, with the SDs of the mean differences ranging from 14.5 to 31.6 cm.

By comparison, it can be seen that our strict method improved the accuracy of the water level inversion results. Even so, in our results, some abnormal water levels and several relatively large differences occurred between the two missions (Table 2), illustrating that although tailored criteria were taken, some water levels from the GEDI still could not represent the real water levels, which may have been caused by the data product quality (Beck et al., 2020). Annual lake area changes may have also affected the screening of laser footprints over the lake. Therefore, for the next step, the lake-area variations were considered using annual high-resolution optical images. In addition, when the satellites had off-pointing angles, the plane position deviation would also affect the laser altimetry accuracy. Assume that the orbit height of the satellite is approximately H (400 km), the laser-pointing angle is $\varnothing$ with the measurement error $\Delta\varnothing$, and the terrain slope is S, the elevation error (Δh) caused by the satellite pointing angle and terrain surface fluctuations can be approximately expressed using Eq. (4) (Gardner, 1992).

$$\Delta h = H\Delta\varnothing\tan(S+\varnothing) \tag{4}$$

When the off-nadir pointing angle is equal to 6° with a 1″ measurement error, assuming a water slope (s) of 0, the elevation error Δh is equal to 0.204 m. More elevation errors simulated under different conditions are listed in Table 3. When the slope and pointing measurement error were constant, the pointing angle seriously affected the elevation accuracy. To ensure the accuracy of the water surface elevation measurements, data taken at small pointing angles should be selected in future studies.

Similarly, the error in the ATL13 product may have been inherited from ATL03, which primarily contained geolocated ellipsoidal heights for each time-tagged photon event downlinked from the ATLAS sensor. Residual errors in the water-height backscatter model and related algorithms may still influence the accuracies of these values due to specular-backscattered, Lambertian-backscattered, and solar Lambertian-backscattered light from the water surface.

4.2. Factors driving lake water level variations

Our results revealed that the lake level of Qinghai Lake increased by an average annual of approximately 0.24 m/yr from 2018 to 2021; this finding is consistent with the trends demonstrated by the latest studies (Chen and Liao, 2020; Xu et al., 2022). Among them, the largest annual increment of 0.56 m occurred in 2019 (Fig. 13(a)); this increase can be mainly attributed to abnormally high annual precipitation (457.3 mm) over the Qinghai Lake basin in this year. The Qinghai Meteorological Bureau also reported that 2019 was defined as an abnormal "wet year", leading to the continuously increasing runoff of all rivers in the basin and causing the water level of Qinghai Lake to continue to rise. Fig. 17 shows the precipitation changes at Buha station (the Buha River is the longest and largest river in the basin, contributing almost half of the total runoff to the lake (Zhang et al., 2011)). In the study area, precipitation months are mainly concentrated from July to September, further explaining why the relatively high-water levels occur mostly in August and September.

Many previous studies have also revealed that over the past half century, the water level of Qinghai Lake presented increasing variations: a rapid increase in the lake area was observed from 2005 to 2016 caused by increased river runoff due to glacier ablation and precipitation (Tang et al., 2018). Fang et al. (2019) demonstrated that the major cause of water level changes (93.13 %) was the combined effect of precipitation and evaporation during the 1960–2016 period, while catchment modifications induced by human activities were very limited during this period (6.87 %). Using a meteorological dataset collected from 1991 to 2017, Chen et al. (2022) indicated that precipitation has the greatest impact on the water volume variations of Qinghai Lake, followed by the accumulated temperature and evaporation. Fan et al. (2021) investigated the abnormal changes from 1970 to 2018 and revealed that the rapid water-level recovery observed in recent years can be attributed to the substantial increases in several key abnormal wet years, such as 2005, 2012, 2015, 2017 and 2018. The lake level variations coincide with annual precipitation rather than temperature or evaporation.

However, seasonal variations in lake levels and the spatial trend patterns differ considerably among different parts of the whole TP, and the factors driving lake distribution dynamics are still under debate (Phan et al., 2013). One viewpoint supports that increasing precipitation was the primary driver behind the rapid expansion of the lake, and permafrost degradation may have contributed a significant amount of water to accelerate the continuous lake expansion in the endorheic basin in recent years (Liu et al. 2021). Pang et al. (2021) showed that the rapid increase in the water volumes of closed lakes over different subzones of the TP could be used to partly explain the observed spatial and temporal heterogeneities of precipitation and temperature. Therefore, in further studies, the use of additional available data, such as direct precipitation, snow melt, glacial melt, moisture condition, evaporation and rainwater runoff data, would promote our further understanding of the driving factors of lake dynamics and global climate change over the TP.

Table 3
The corresponding range error/m caused by satellite slant angle and pointing measurement error.

Off-nadir (°)/Uncertainty (″)	Slop(°)			
	0	0.5	1	1.5
6/2.5	0.509	0.552	0.595	0.638
5/2.5	0.424	0.467	0.509	0.552
4/2.5	0.339	0.381	0.424	0.467
3/2.0	0.203	0.237	0.271	0.305
2/1.5	0.102	0.127	0.152	0.178
1/1.0	0.034	0.051	0.068	0.085

5. Conclusion

Obtaining accurate lake level fluctuations is necessary for solving the high uncertainties regarding the water balance of the Tibetan Plateau basin. Lakes located in this region are surrounded by high-elevation, rough terrain, the surface environment of which varies seasonally, and it is more difficult to measure the dynamics of these lakes than of lakes elsewhere. New altimetry satellites provide a solution for monitoring water level changes in areas without *in situ* gauging data.

In this study, the recent water level dynamics of Lake Qinghai are examined by integrating refined ICESat-2 and GEDI data. A tailored scheme is implemented to refine the raw data products first, and then the factors that affected the accuracy of the GEDI data were analyzed. The ICESat-2 laser altimetry data exhibit a strong capability for monitoring the lake level with a very high accuracy. The GEDI dataset has a dense temporal advantage and can monitor the lake level for a maximum of 8 days in a month, though the accuracy of these data is inferior to that of the ICESat-2 data, and large differences exist among different beams, most of which overestimated the water levels by 0.264 ± 0.357 m. The availability of the GEDI algorithm-2 footprints was higher than that of the algorithm 1 footprints, and beams 1 and 2 were recommended for further application. Compared to the results obtained from the DAHITI dataset, the accuracy of our integrated results still needs to be further improved, and the factors affecting the accuracy extraction, such as the slant angle and pointing measurement error of the GEDI data, need to be further investigated.

Our integrated results, the *in situ* measurements, the DAHITI dataset, and the Hydroweb dataset demonstrate increase rates ranging from 0.243 to 0.367 m/yr during the 2018 to 2021 period. The relatively high-water-level periods are distributed mostly in August and September, followed by in October and November, while the lower-water-level periods are distributed mostly in February and March. The main driving factor inducing high water levels was surging annual precipitation, especially in 2019. The inter-year and intra-year comparisons between the above four sources showed that the validation of our results and the intra-year changes in 2019 with relatively rich observation data over all 12 months were strongly consistent with the *in situ* lake-level measurements, with a difference of 0.03 m; this finding confirms that the constructed long-time-series lake-level dataset allows us to capture the monthly, seasonal, and annual cycles of lake level variations and can serve as a valuable tool for hydrological and climatic studies when hydrological station-measured data are lacking. Comprehensive examinations of lake level changes will become possible once rich GEDI and ICESat-2 data become available in the next few years.

Funding

This research was funded by the Open Fund of State Key Laboratory of Remote Sensing Science (Grant No. OFSLRSS202111) and Strategic Priority Research Program Project of the Chinese Academy of Sciences (Grant No. XDA23040100).

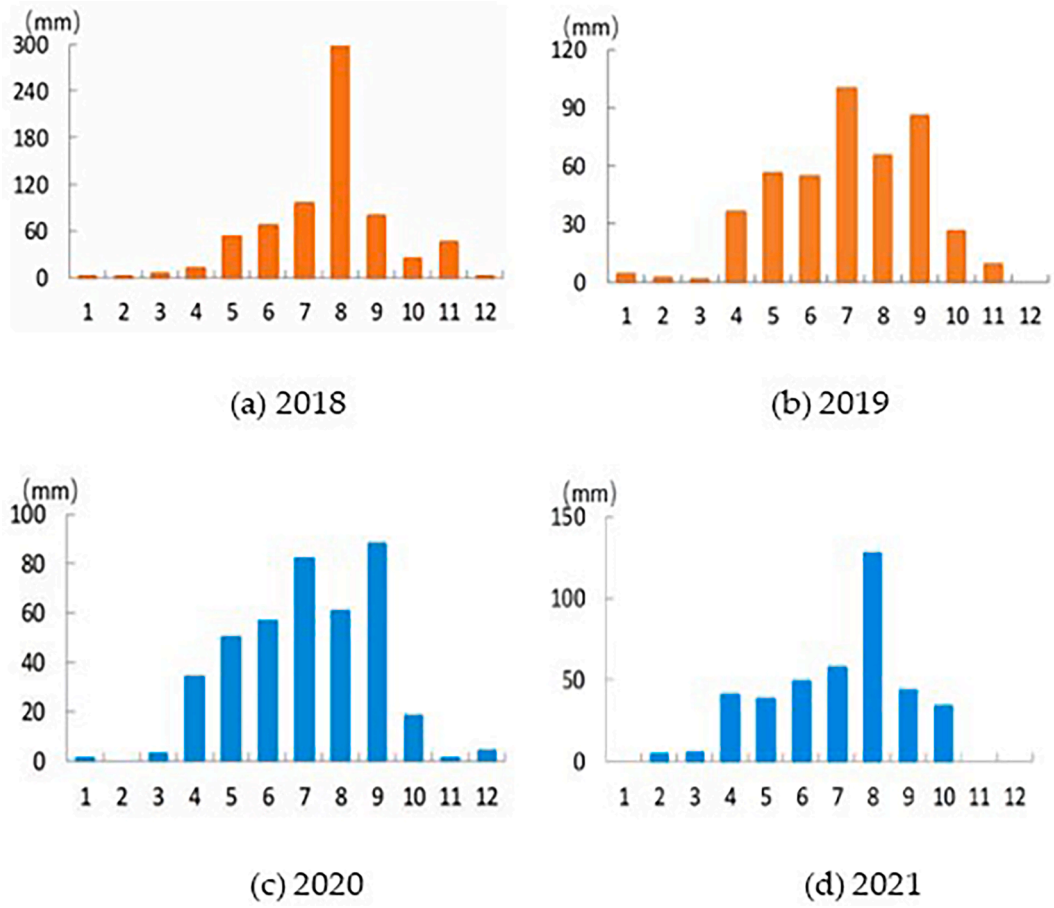

Fig. 17. Average monthly precipitation of Qinghai Lake (The vertical axis is the precipitation, and the horizontal axis is the month (the figures were quoted from the Qinghai Lake Water Resources Bulletin https://slt.qinghai.gov.cn/subject?cid=24)): (a) 2018; (b) 2019; (c) 2020; (d) 2021.

CRediT authorship contribution statement

Zhijie Zhang: Conceptualization, Methodology, Software, Formal analysis, Data curation, Writing – original draft, Writing – review & editing. **Yanchen Bo:** Methodology, Validation. **Shuanggen Jin:** Conceptualization, Formal analysis, Writing – review & editing. **Guodong Chen:** Software, Writing – review & editing. **Zhounan Dong:** Software, Visualization.

Declaration of Competing Interest

The authors declare that they have no known competing financial interests or personal relationships that could have appeared to influence the work reported in this paper.

Data availability

The GEDI and ICESat-2 data that support the findings of this study are available in [Earthdata Search (nasa.gov)]. The other two lake level public datasets were derived from the following resources available in the public domain: [https://hydroweb.theia-land.fr/hydroweb] and [https://dahiti.dgfi.tum.de/en/].

Acknowledgments

Authors would thank Xiaozu Guo and Minqin He for data curation and the GEDI team and the NASA LPDAAC (Land Processes Distributed Active Archive Center) for providing GEDI data as well as the National Snow and Ice Data Center for providing ICESat-2 ATL13 dataset.

References

Adam, M., Urbazaev, M., Dubois, C., Schmullius, C., 2020. Accuracy assessment of GEDI terrain elevation and canopy height estimates in European temperate forests: Influence of environmental and acquisition parameters. Remote Sens. 12, 3948.

Beck, J., Armston, J., Hofton, M., Luthcke, S.J.S.F., South Dakota, USA: EROS Center, US Geological Survey, 2020. Global Ecosystem Dynamics Investigation (GEDI) Level 02 User Guide.

Birkett, C.M., Beckley, B., 2010. Investigating the performance of the Jason-2/OSTM radar altimeter over lakes and reservoirs. Mar. Geod. 33 (S1), 204–238.

Bosch, W., Dettmering, D., Schwatke, C., 2014. Multi-mission cross-calibration of satellite altimeters: Constructing a long-term data record for global and regional sea level change studies. Remote Sens. 6 (3), 2255–2281.

Busker, T., Roo, A.d., Gelati, E., Schwatke, C., Adamovic, M., Bisselink, B., Pekel, J.-F., Cottam, A., 2019. A global lake and reservoir volume analysis using a surface water dataset and satellite altimetry. Hydrol. Earth Syst. Sci. 23(2), 669–690.

Calmant, S., Seyler, F., Cretaux, J.F., 2008. Monitoring continental surface waters by satellite altimetry. Surv. Geophys. 29 (4), 247–269.

Chen, J., Liao, J., 2020. Monitoring lake level changes in China using multi-altimeter data (2016–2019). J. Hydrol. 590, 125544.

Chen, Q., Liu, W., Huang, C., 2022. Long-Term 10 m Resolution Water Dynamics of Qinghai Lake and the Driving Factors. Water 14 (4), 671.

Crétaux, J.-F., Calmant, S., Del Rio, R.A., Kouraev, A., Bergé-Nguyen, M., Maisongrande, P., 2011. Lakes studies from satellite altimetry, Coastal Altimetry. Springer 509–533.

Dandabathula, G., Rao, S., 2020. Validation of ICESat-2 surface water level product ATL13 with near real time gauge data. Hydrol. 8 (2), 19–25.

Dubayah, R., Blair, J.B., Goetz, S., Fatoyinbo, L., Hansen, M., Healey, S., Hofton, M., Hurtt, G., Kellner, J., Luthcke, S., 2020. The Global Ecosystem Dynamics Investigation: High-resolution laser ranging of the Earth's forests and topography. Sci. Remote Sens. 1, 100002.

Fan, C., Song, C., Li, W., Liu, K., Cheng, J., Fu, C., Wang, J., 2021. What drives the rapid water-level recovery of the largest lake (Qinghai Lake) of China over the past half century? J. Hydrol. 593, 125921.

Fang, J., Li, G., Rubinato, M., Ma, G., Zhou, J., Jia, G., Wang, H., 2019. Analysis of long-term water level variations in Qinghai Lake in China. Water 11 (10), 2136.

Fayad, I., Baghdadi, N., Bailly, J.S., Frappart, F., Zribi, M., 2020. Analysis of GEDI elevation data accuracy for inland waterbodies altimetry. Remote Sens. 12 (17), 2714.
Fayad, I., Baghdadi, N.N., Alvares, C.A., Stape, J.L., Bailly, J.S., Scolforo, H.F., Zribi, M., Le Maire, G., 2021. Assessment of GEDI's LiDAR data for the estimation of canopy heights and wood volume of eucalyptus plantations in Brazil. IEEE J. Sel. Top. Appl. Earth Obs. Remote Sens. 14, 7095–7110.
Frappart, F., Biancamaria, S., Normandin, C., Blarel, F., Bourrel, L., Aumont, M., Azemar, P., Vu, P.-L., Le Toan, T., Lubac, B., 2018. Influence of recent climatic events on the surface water storage of the Tonle Sap Lake. Sci. Total Environ. 636, 1520–1533.
Frappart, F., Blarel, F., Fayad, I., Bergé-Nguyen, M., Crétaux, J.-F., Shu, S., Schregenberger, J., Baghdadi, N., 2021. Evaluation of the Performances of Radar and Lidar Altimetry Missions for Water Level Retrievals in Mountainous Environment: The Case of the Swiss Lakes. Remote Sens. 13 (11), 2196.
Gardner, C.S., 1992. Ranging performance of satellite laser altimeters. IEEE Trans. Geosci. Remote Sens. 30 (5), 1061–1072.
Ghashghaie, M., Eslami, H., Ostad-Ali-Askari, K., 2022. Applications of time series analysis to investigate components of Madiyan-rood river water quality. Appl. Water Sci. 12 (8), 1–14.
Guo, J., Chang, X., Gao, Y., Sun, J., Hwang, C., 2009. Lake level variations monitored with satellite altimetry waveform retracking. IEEE J. Sel. Top. Appl. Earth Obs. Remote Sens. 2 (2), 80–86.
Hofton, M., Blair, J., Story, S., Yi, D., 2019. Algorithm Theoretical Basis Document (ATBD) for GEDI transmit and receive waveform processing for L1 and L2 products. Goddard Space Flight Centre.
Hui, Z., Hu, Y., Jin, S., Yevenyo, Y.Z., 2016. Road centerline extraction from airborne LiDAR point cloud based on hierarchical fusion and optimization. ISPRS J. 118, 22–36.
Jasinski, M., Stoll, J., Hancock, D., Robbins, J., Nattala, J., Pavelsky, T., Morrison, J., Arp, C., Jones, B., Ondrusek, M.J.G.S.F.C.G., MD, USA, 2019. Algorithm Theoretical Basis Document (ATBD) for Inland Water Data Products ATL13 Version 1.
Javadinejad, S., Eslamian, S., Ostad-Ali-Askari, K., 2019. Investigation of monthly and seasonal changes of methane gas with respect to climate change using satellite data. Appl. Water Sci. 9 (8), 180.
Kleinherenbrink, M., Ditmar, P., Lindenbergh, R., 2014. Retracking Cryosat data in the SARIn mode and robust lake level extraction. Remote Sens. Environ. 152, 38–50.
Kropáček, J., Braun, A., Kang, S., Feng, C., Ye, Q., Hochschild, V., 2012. Analysis of lake level changes in Nam Co in central Tibet utilizing synergistic satellite altimetry and optical imagery. J. Appl. Earth Obs. Geoinf. 17, 3–11.
Lawford, R., Strauch, A., Toll, D., Fekete, B., Cripe, D., 2013. Earth observations for global water security. Curr. Opin. Environ. Sustain. 5 (6), 633–643.
Li, P., Li, H., Chen, F., Cai, X., 2020. Monitoring long-term lake level variations in middle and lower Yangtze basin over 2002–2017 through integration of multiple satellite altimetry datasets. Remote Sens. 12 (9), 1448.
Liu, W., Xie, C., Zhao, L., Li, R., Liu, G., Wang, W., Liu, H., Wu, T., Yang, G., Zhang, Y., 2021. Rapid expansion of lakes in the endorheic basin on the Qinghai-Tibet Plateau since 2000 and its potential drivers. Catena 197, 104942.
Luo, S., Song, C., Zhan, P., Liu, K., Chen, T., Li, W., Ke, L., 2021. Refined estimation of lake water level and storage changes on the Tibetan Plateau from ICESat/ICESat-2. Catena 200, 105177.
Neumann, T., Brenner, A., Hancock, D., Robbins, J., Saba, J., Harbeck, K., Gibbons, A., Lee, J., Lutchke, S., Rebold, T., 2020. Algorithm Theoretical Basis Document (ATBD) for Global Geolocated Photons (ATL03). Goddard Space Flight Center, Release, p. 003.
Pang, S., Zhu, L., Yang, R., 2021. Interannual Variation in the Area and Water Volume of Lakes in Different Regions of the Tibet Plateau and Their Responses to Climate Change. Front. Earth Sci. 943.
Phan, V.H., Lindenbergh, R., Menenti, M., 2012. ICESat derived elevation changes of Tibetan lakes between 2003 and 2009. Int. J. Appl. Earth Obs. Geoinf. 17, 12–22.
Phan, V., Lindenbergh, R., Menenti, M., 2013. Geometric dependency of Tibetan lakes on glacial runoff. Hydrol. Earth Syst. Sci. 17 (10), 4061–4077.
Roy, D.P., Kashongwe, H.B., Armston, J., 2021. The impact of geolocation uncertainty on GEDI tropical forest canopy height estimation and change monitoring. Sci. Remote Sens. 4, 100024.
Schwatke, C., Dettmering, D., Bosch, W., Seitz, F., 2015. DAHITI–an innovative approach for estimating water level time series over inland waters using multi-mission satellite altimetry. Hydrol. Earth Syst. Sci. 19 (10), 4345–4364.
Song, C., Huang, B., Ke, L., Richards, K.S., 2014. Seasonal and abrupt changes in the water level of closed lakes on the Tibetan Plateau and implications for climate impacts. J. Hydrol. 514, 131–144.
Talebmorad, H., Ahmadnejad, A., Eslamian, S., Ostad-Ali-Askari, K., Singh, V.P., 2020. Evaluation of uncertainty in evapotranspiration values by FAO56-Penman-Monteith and Hargreaves-Samani methods. Int. J. Hydrol. Sci. Technol. 10 (2), 135–147.
Talebmorad, H., Ostad-Ali-Askari, K., 2022. Hydro geo-sphere integrated hydrologic model in modeling of wide basins. Sustain. Water Resour. Manag. 8 (4), 1–17.
Tang, L., Duan, X., Kong, F., Zhang, F., Zheng, Y., Li, Z., Mei, Y., Zhao, Y., Hu, S., 2018. Influences of climate change on area variation of Qinghai Lake on Qinghai-Tibetan Plateau since 1980s. Sci. Rep. 8, 1–7.
Tian, X., Shan, J., 2021. Comprehensive evaluation of the ICESat-2 ATL08 terrain product. IEEE Trans. Geosci. Remote Sens. 59 (10), 8195–8209.
Velpuri, N., Senay, G.B., Asante, K., 2012. A multi-source satellite data approach for modelling Lake Turkana water level: calibration and validation using satellite altimetry data. Hydrol. Earth Syst. Sci. 16 (1), 1–18.
Wang, H., Chu, Y., Huang, Z., Hwang, C., Chao, N., 2019. Robust, long-term lake level change from multiple satellite altimeters in Tibet: Observing the rapid rise of Ngangzi Co over a new wetland. Remote Sens. 11 (5), 558.
Xiang, J., Li, H., Zhao, J., Cai, X.D., Li, P., 2021. Inland water level measurement from spaceborne laser altimetry: Validation and comparison of three missions over the Great Lakes and lower Mississippi River. J. Hydrol. 597, 126312.
Xu, F., Zhang, G., Yi, S., Chen, W., 2022. Seasonal trends and cycles of lake-level variations over the Tibetan Plateau using multi-sensor altimetry data. J. Hydrol. 604, 127251.
Yuan, C., Gong, P., Bai, Y., 2020. Performance assessment of ICESat-2 laser altimeter data for water-level measurement over lakes and reservoirs in China. Remote Sens. 12 (5), 770.
Yue, H., Liu, Y., Wei, J., 2021. Dynamic change and spatial analysis of Great Lakes in China based on Hydroweb and Landsat data. Arabian J. Geosci. 14 (3), 1–17.
Zhang, G., Xie, H., Duan, S., Tian, M., Yi, D., 2011. Water level variation of Lake Qinghai from satellite and in situ measurements under climate change. J. Appl. Remote Sens. 5 (1), 053532.
Zhang, G., Chen, W., Xie, H., 2019. Tibetan Plateau's lake level and volume changes from NASA's ICESat/ICESat-2 and Landsat Missions. Geophys. Res. Lett. 46 (22), 13107–13118.
Zhao, Y., Liao, J., Shen, G., Zhang, X., 2017. Monitoring the water level changes in Qinghai Lake with satellite altimetry data (in Chinese). J. Remote Sens. 21 (4), 633–644.